Deepening of the Atlantic Water Core in the Canada Basin in 2003–11

WENLI ZHONG AND JINPING ZHAO

Key Lab of Physical Oceanography, Ocean University of China, Qingdao, China

(Manuscript received 23 April 2013, in final form 26 May 2014)

ABSTRACT

In 2004, a cold mode of Atlantic Water (AW) entered the western Canada basin, replacing the anomalously warm AW that resided in the basin since the 1990s. This slightly colder AW was denser than the 1990s warm mode; it gradually filled most of the western basin by 2009. The enhanced surface stress curl led to the spinup of the Beaufort Gyre and convergence of freshwater. The spinup also resulted in a deepening of the AW core at the center of the gyre and in shoaling of the AW core at the margins of the gyre. The density versus depth relationship revealed in this study shows that the depth of the maximum AW temperature was mainly controlled by the density structure before 2007; thus, it is the case when the denser water was deeper and the case when the lighter water was shallower around the basin. However, this relationship was reversed to become the case when the denser water was shallower and the case when the lighter water was deeper since 2008 inside the Beaufort Gyre. The combined effect of density and sea ice retreat that enhanced surface stress curl determined the depth of the AW inside the Beaufort Gyre since 2008. The deepening of the AW core and expanding of the area where the AW deepening occurred had a profound effect on the large-scale circulation in the Arctic Ocean.

1. Introduction

The core layer of the Atlantic Water (AW) in the Arctic Ocean (depth range about 150 to 900 m) is originated from the North Atlantic Ocean. The AW is composed of warm, saline water from the Fram Strait branch (FSB; 0.4 ~ 2.2°C, 34.77 ~ 34.91) and colder, fresher water from the Barents Sea branch (BSB; −0.2° ~ 0.55°C, 34.83 ~ 34.93) (Schauer et al. 1997, 2002). As part of the circumpolar boundary current, the AW flows cyclonically along the continental slope (Rudels et al. 1999; Aksenov et al. 2011). The driving mechanism for the boundary current is not yet fully understood. Some studies suggested that the balance of potential vorticity may determine the cyclonic circulation of the AW (e.g., Yang 2005; Aksenov et al. 2011). A seasonal signal of the AW was identified in the Nansen basin and divided into "summer" (warmer and saltier) and "winter" (colder and fresher) types (Dmitrenko et al. 2009; Ivanov et al. 2009). The seasonal variations of temperature and salinity are pronounced in the Nansen basin (Ivanov et al. 2009), while in the western Laptev Sea, near the North Pole and in the Canada basin, observations show no evidence of the seasonal cycle in the temperature of the AW core (Lique and Steele 2012).

Analyzing the simulated annual sea ice motion and ocean circulation in the Arctic Ocean, Proshutinsky and Johnson (1997) revealed two circulation regimes: cyclonic and anticyclonic alternating at intervals of 5–7 yr with a period of 10–15 yr. In the cyclonic (anticyclonic) regime, warmer (colder) AW inflow enters the Arctic Ocean, and the anticyclonic Beaufort Gyre (BG) weakens (strengthens), with a divergence (convergence) of surface current and shoaling (depression) of the AW (Polyakov et al. 2004). In the early 1990s, a maximum temperature of the FSB water was observed to be ~1°C higher than the climatological record in the Nansen basin (Quadfasel et al. 1991). This anomalously warm AW reached the western edge of the Canada basin in 1999 (Zhao et al. 2005) and began to spread into the basin gradually (Shimada et al. 2004a; McLaughlin et al. 2005, 2009). Recent studies show that the warming of the AW in the Canada basin is not a monotonic process; instead, it consists of warm pulses of the AW entering the Arctic Ocean through Fram Strait and propagating downstream in the Arctic Ocean (Polyakov et al. 2005, 2011).

The AW contains a large heat content in the Arctic Ocean; it has a great impact on the heat balance of the ocean and the AW warming helped precondition the

Corresponding author address: Wenli Zhong, Key Lab of Physical Oceanography, Ocean University of China, 238 Songling Road, Qingdao, 266100, China.
E-mail: wlzhongouc@163.com; jpzhao@ouc.edu.cn

DOI: 10.1175/JPO-D-13-084.1

extreme sea ice retreat of recent years (Zhang et al. 1998; Polyakov et al. 2010). The AW loses its heat as it travels through the Arctic basin and simultaneously the Atlantic Water core depth (AWCD) increasing. The AW loses most of its energy as it flow along the Eurasian continental slope, while this process tapers off in the Canada basin. The depth variation of the AW core is preconditioned by the maximum temperature of AW that flows into the basin. For a certain water mass, the variation of temperature will result in the change of density, and for a subsurface geostrophic current, the water mass will flow along an isopycnal interface (Iselin's conceptual model; Iselin 1939). The water mass has to move to its relevant isopycnal as its density changes, which results in the change of the AWCD. The 1990s anomalously warm AW brought in not only warmer water but also the shoaling effect of the AW core. In the 1990s, the AWCD in the western Arctic Ocean decreased by approximately 150 m (Polyakov et al. 2004) compared to the 1970s (Carmack et al. 1997; Swift et al. 1997). Hydrological observations showed that the AWCD shoaled by ~50 m in 2002 compared to that in 1997/98 in the southern Canada basin (McLaughlin et al. 2005). These results indicate that the variability of the AWCD is synchronized to some extent with temperature. A significant reduction of AW temperature may be caused by four factors: the influence of mixing with shelf waters (Lenn et al. 2009), much stronger interaction between the atmosphere and the ocean as more ice-free area ventilates the ocean's interior (Polyakov et al. 2011), the presence of eddies that enhanced the vertical heat flux from the AW (e.g., Lique et al. 2014), and the cooling phase of the AW. In the central Canada basin, the double-diffusive staircase acts as a barrier to prevent the heat exchange between the AW layer and the upper ocean (Timmermans et al. 2008). So the reduction of AW temperature there may be due to the cooling phase of the AW inflow. When the AW in the western Mendeleev Ridge is colder than that in the Chukchi Borderland region (Woodgate et al. 2007), a slightly colder AW is on its way to transport into the Canada basin through the circumpolar boundary current.

Studies have shown an increasing freshwater content in the upper ocean of the Canada basin (e.g., McPhee et al. 2009; Proshutinsky et al. 2009; Giles et al. 2012) and the spinup of the Beaufort Gyre (McLaughlin et al. 2011; Giles et al. 2012) in an anticyclonic regime for at least 14 yr. Here, we investigate recent variability of the AWCD in the Canada basin during the slightly colder AW (comparing to the 1990s warm anomaly) in a period that favors the anticyclonic regime in the Canada basin. Impacts of AW cooling and the surface stress curl on changes of AW depth are explored.

2. Data and method

a. Hydrography

Temperature and salinity profile data were collected and made available by the Beaufort Gyre Exploration Project (BGEP) at the Woods Hole Oceanographic Institution (www.whoi.edu/beaufortgyre), in collaboration with researchers from Fisheries and Oceans Canada at the Institute of Ocean Sciences (2003–11) (McLaughlin et al. 2008). We also use the hydrographic data from the Japan Agency for Marine–Earth Science and Technology (JAMSTEC) Research Vessel (R/V) *Mirai* (www.godac.jamstec.go.jp/darwin/datatree/e) in 2004, 2008, and 2009 (Shimada et al. 2004b) and from the Chinese Arctic Research Expedition (see CHINARE data from 2003, 2008, and 2010). [The CHINARE data are issued by the data-sharing platform of polar science (http://www.chinare.org.cn) maintained by the Polar Research Institute of China (PRIC) and Chinese National Arctic and Antarctic Data Center (CN-NADC).] The entire survey was carried out in the time range of late July to early October, which could represent the summer condition of the Canada basin. All data from the stations with deployment depth greater than 1000 m are used. The maximum potential temperature of AW was chosen to determine the AWCD. The data from profiling instruments at the bottom-anchored mooring system [McLane Moored Profiler (MMP)] acquired by the Beaufort Gyre Observational System (BGOS; www.whoi.edu/page.do?pid=66559) are analyzed to study the interannual change of the AW. The MMP data acquisition followed a burst sampling scheme consisting of two one-way profiles separated in time by 6 h and initiated every 48 h. The MMP salinity data are believed to have an uncertainty of less than 0.005 (Ostrom et al. 2004).

b. Sea ice concentration

The sea ice concentration data are from the AMSR–EASI ice concentration dataset, which has a grid size of 6.25 km × 6.25 km (Spreen et al. 2008). (The data are available online at http://iup.physik.uni-bremen.de:8084/amsr/amsre.html.)

c. Atmospheric conditions and sea ice motion

Daily mean sea level pressure over the Arctic Ocean was derived from the National Centers for Environmental Prediction–National Center for Atmospheric Research (NCEP–NCAR) reanalysis dataset (Kalnay et al. 1996). The horizontal resolution of the data is 2.5° × 2.5°. (The data are available at www.esrl.noaa.gov/psd/data/gridded/). Daily sea ice motion data were derived from the Polar Pathfinder Daily 25-km EASE-Grid Sea Ice Motion Vectors (Fowler et al. 2013) for the period from 1978 to 2012 with a resolution of 25 km.

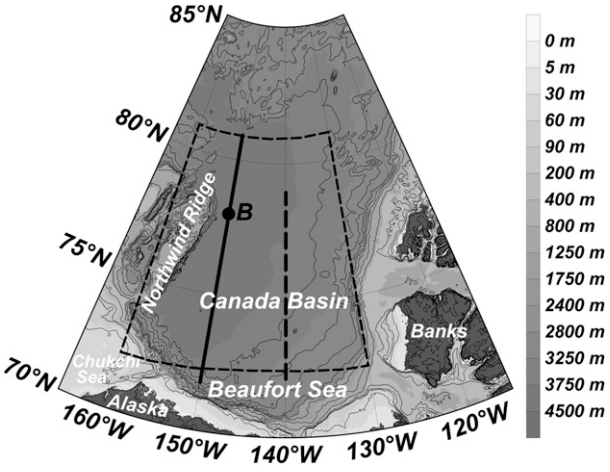

FIG. 1. Bathymetry of the Canada basin, based on the data from the International Bathymetric Chart of the Arctic Ocean (IBCAO). Mooring B is indicated by the black dot. The solid and dashed lines mark the western and eastern sections, respectively. The defined Canada basin area (72°–81°N, 130°–160°W) that was used to calculate the mean surface stress curl is shown by a dashed line contour.

(The data are available at http://nsidc.org/data/nsidc-0116.html.)

The wind stress was calculated from the sea level pressure (daily) following a formulation adopted in the Arctic Ocean Model Intercomparison Project (AOMIP). The surface stress over the sea ice–covered ocean was also calculated based on the sea ice motion data. Using the wind stress and ice–ocean stress, we then calculate the total stress on each grid based on the sea ice concentration as suggested by Yang (2009). Daily surface stress curl was calculated based on the total stress and then averaged to obtain the monthly-mean fields; the latter are used for analysis. All the primary data were interpolated on the EASE grid with a resolution of 25 km.

3. Deepening of the AW core and expanding of the area where the AW deepening occurred

There is evidence that when the anomalously warm AW arrives in the Canada basin, the AWCD becomes shallower (McLaughlin et al. 2002, 2005; Polyakov et al. 2004). When the warming phase was over, the warm AW was followed by a slightly colder AW. MMP mooring B is located east of the northeastern Northwind Ridge (Fig. 1), near the main gateway of the AW into the basin. The mooring data show a cooling trend of the AW since 2004 (Fig. 2) accompanied by a deepened AW core. The decline of AW core temperature was ~0.2°C, and the decline of salinity was ~0.01 PSU during 2004–09, while the deepening of the AW core was ~70 m. The coefficient of thermal expansion $\alpha = -\partial\rho/(\rho\partial\theta)$ is small compared to the haline contraction coefficient $\beta = \partial\rho/(\rho\partial S)$, and the ratio of these two parameters is $\alpha/\beta \approx 0.1$ in the Arctic Ocean (Zhang and Zhao 2007). So the ratio of the contribution from temperature (~0.2°C) and salinity (~0.01 PSU) to the density here is $\Delta\rho_t/\Delta\rho_s \approx 2$; this means that the density change here is mainly due to temperature change. Since the heat transport from the AW to the upper ocean is very small (less than 1 W m^{-2}) in the central Canada basin (Timmermans et al. 2008), this cooling is speculated to be a transport result of a cold phase of the AW. The presence of eddies is an effective mechanism to enhance the vertical heat flux from the AW (e.g., Lique et al. 2014). Mooring B does show the presence of some eddies during 2003–09, but much less than mooring A (see Fig. 3 of Lique et al. (2014)). Most eddies are cold-core, anticyclonic eddies that present in the subsurface layer shallower than the depth of AW. Those eddies only last for 1 or 2 days. In terms of the overall trend during 2003–09, the inflow of slightly colder AW is the main factor for the cooling trend in mooring B. The effect of eddies to the overall trend of interannual AW variation should be evaluated by whether the numbers of eddies increased or intensified, which requires further investigation.

On reaching the northeastern Chukchi Borderland, the boundary current bifurcates into two branches. One branch flows along the Northwind Ridge to the south and merges with the boundary current there, then continues to flow eastward along the Beaufort shelf (Woodgate et al. 2007; McLaughlin et al. 2009), while the other flows to the east and enters the Canada basin (Shimada et al. 2004a), which is in the form of thermohaline intrusion under the influence of the Beaufort Gyre (McLaughlin et al. 2009).

The slightly colder AW started to spread in the Canada basin in 2004. The spreading is found to be very complex, as the slightly colder water arrived at different areas at different time. The reality is that the cooling occurred in the upstream area, while the warming continued in the downstream area. At the same time, the AWCD exhibited complex spatial variation associated with the AW temperature variation over the basin as described in some recent literature (e.g., Polyakov et al. 2004; McLaughlin et al. 2005).

The AWCD is easy to detect from the CTD data as the remarkable high temperature of the AW. The horizontal isolines of AWCD could reveal regions with deepened or shoaled AW. In this study, we focus on the expanding of the area where the AW deepening occurred in the basin and its main dynamic mechanisms, ignoring the complex variability of the AWCD in the specific area. An AWCD isoline was chosen as the arbitrary border between the deep and shallow AWCD

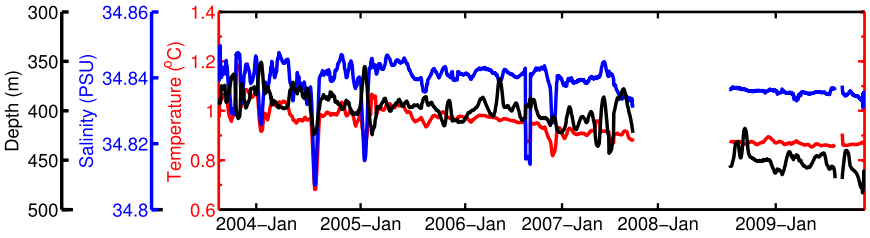

FIG. 2. The temperature, salinity, and depth of the AW core from McLane Moored Profiler at mooring B (78°N, 150°W). An 11-day running average is applied to the original data. The record shows missing data during late 2007 and 2008.

regions. The movement of the isoline in time indicates the spatially expanding and contracting processes of the area where the AW deepening occurred. The isolines of 400–420 m are all qualified to be the indicator (figures not shown), as the AWCD in 2003 was less than 400 m in most survey area of the Canada basin, but by the year 2009, it was deeper than 420 m around most of the area. Therefore, in this study, the 410-m isoline was chosen.

In 2003, the AWCD was less than 410 m in almost the entire survey area of the Canada basin except for the southeastern corner (larger than 450 m; Fig. 3). Since 2004, the 410-m isoline began to extend toward the west. The isoline reached the Northwind Ridge, forming an east–west extending zone with deepened AW core, in 2005 and 2006. Since 2007, the deepened AW core region started to expand northward along the Northwind Ridge. The deepened AW core region continued to expand and reached north of 80°N by 2008. Most of the survey area of the Canada basin was filled by the deepened AW core in 2009.

It is an obvious transition in the Canada basin, from the nearly entirely shallow AWCD in 2003 to the nearly entirely deepened AW core in 2009. As the Arctic sea ice and ocean have been experiencing rapid changes since the end of the last century, the transition of AWCD could be an important component of the changing Arctic. As the deepening of the AW core is still ongoing, we try to discuss the main driving factors in this study, in order to understand the transition mechanism of the AWCD.

a. Deepening of the AW core contributed by cooling of AW

The temperature of the AW off the northeastern corner of the Chukchi Borderland reached its highest in 2003 (Figs. 2, 4), which is considered an upstream source of the AW in the Canada basin. Since then, the source temperature was decreasing gradually, while the anomalous warm AW was still spreading into the basin (Fig. 4). Therefore, the temperature should vary in different ways in the western and eastern parts of the basin. Here, we choose two sections with multiyear surveys in the Canada basin, as shown in Fig. 1, where the solid and dashed lines mark the ''western section'' and ''eastern section,'' respectively.

The western section shows that the maximum AW temperature appeared north of 77°N, which is the pathway of the warm AW entering the Canada basin through thermohaline intrusion (McLaughlin et al. 2009). The maximum temperature area (temperature $>$ 0.85°C) remained in the northern part of the section (north of 75°N) and did not seem to spread to the south along this section (Fig. 5; dashed contour area). The maximum value of the AW temperature decreased year by year after 2007. The high temperature area (temperature $>$ 0.85°C) nearly vanished in 2009 and 2011. It indicates that the source water transported by the bifurcated branch of the AW had been cooled down from 2003 to 2011, and the slightly colder water was becoming dominant in the western section. Also notice the bowl shape of 0°C isotherm since 2008 that could represent the interface between the Pacific-derived water and AW.

Contrary to the western section, the AW temperature in the eastern section did not show any significant cooling; instead, it indicates some expanding of the warm-water area (Fig. 6). The warm center in 2003 appeared north of 77°N and at the depth of about 370 m. The warm area (temperature $>$ 0.75°C) along this section then extended to the south after 2003 and reached its southernmost location in 2009 with the core depth at about 450 m. Although the warm-water area of the AW was expanding, the maximum temperature of the AW did not show any significant increase, but rather was stable from 2006 to 2008 and then gradually decreased after 2008. The maximum temperature of the AW in the eastern section is lower compared to that in the western section during the same period. It indicates a delayed arrival of anomalously warm AW in the basin.

Therefore, the overall situation during 2003–09 was that a significant cooling appeared in the west, while the warm-water area of the AW expanded (with a rather stable maximum temperature of the AW in 2006–08 and gradual decrease after 2008) east of the Canada basin. It

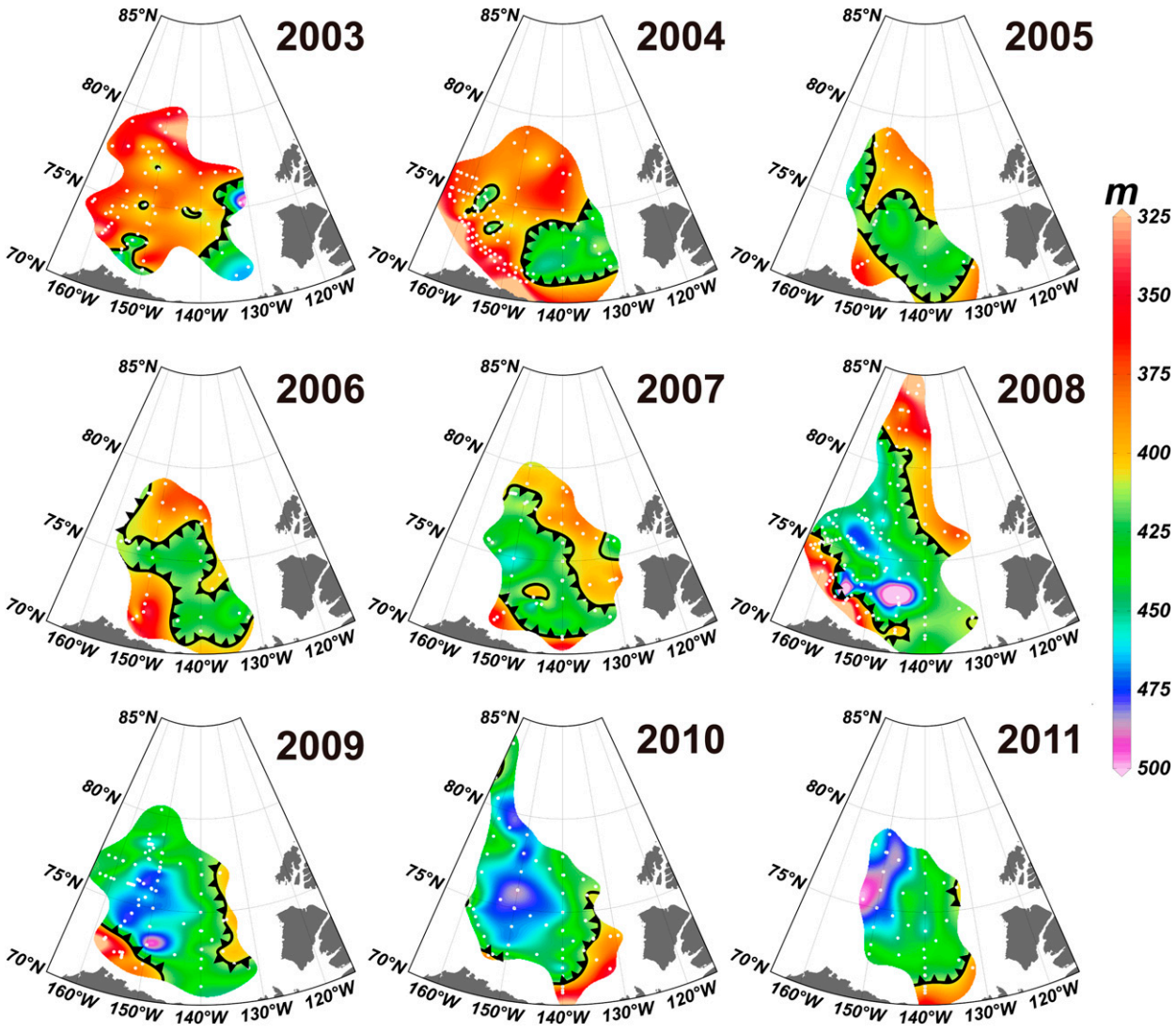

FIG. 3. Expansion of the area where the AW deepening occurred (AWCD; shading). The white dots indicate the locations where the CTD data were collected. The irregular black line marks the 410-m isoline, with the triangles pointing toward the deeper AWCD.

is interesting that the AWCDs along both sections increased. The cooling of the AW source water would result in a deepened AW core to some extent; the question is whether or not the deepening of the AW core was induced solely by the cooling of the AW.

b. *Deepening of the AW core contributed by dynamic processes*

Besides the effect of the inflow of slightly colder AW, the deepening could also be induced by dynamic processes. Surface divergence/convergence will result in a change in dynamic height, therefore, the change in the depth of the interface between the AW and the upper ocean. Isopycnal is a good indicator for identifying an interface; in other words, not only the change in temperature can alter the depth of isopycnal, but also the change in dynamic height.

Take the 27.92 $kg\,m^{-3}$ isopycnal as a reference interface; it shows a consistent deepening in the western section (Fig. 7). The anticyclonic BG has a bowl shape, with isohalines deeper at the center and shallower at the edge (Proshutinsky et al. 2002). A typical bowl shape appeared in each year as the section was always across part of the BG. The deepest position of the isopycnal should be the closest to the center of the gyre. If the bowl shape becomes deeper, it indicates an enhanced BG and an increased dynamic height. The bowl shape of the isopycnal became deeper after 2005 and reached the deepest in 2009. The difference of isopycnal depths

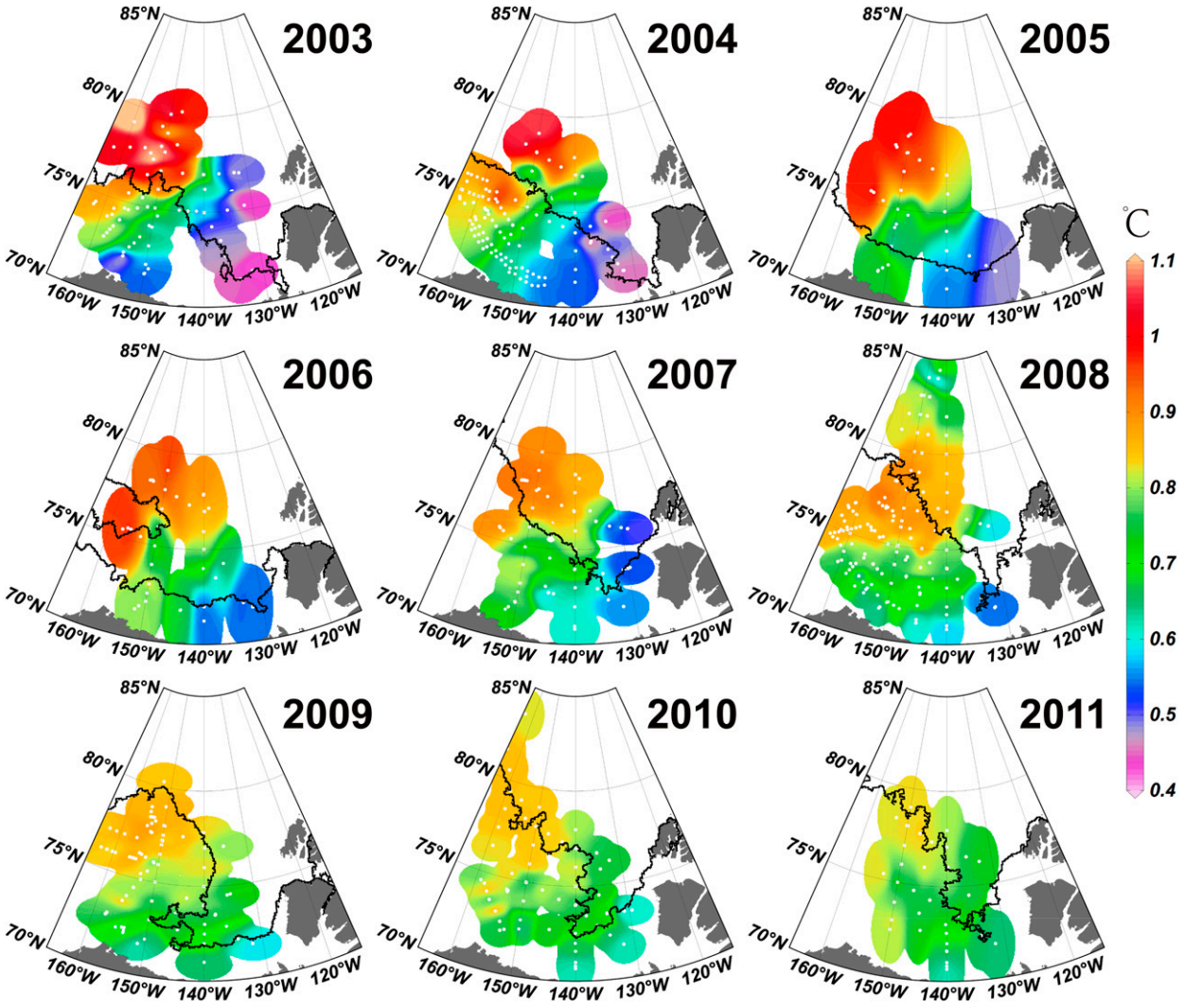

FIG. 4. Multiyear variation of maximum AW temperature and the minimum sea ice edge (black line) for 2003–11. The white dots indicate the locations where the CTD data were collected, and the values between stations are interpolated.

between the center and the margin was about 80 m in 2009, while it was only about 20 m in the eastern section.

The same isopycnal in the eastern section is quite different from that in the western section. In the eastern section, the original isopycnal is a tilted one with the shallow part to the north. Since 2008, the isopycnal was deepening and its slope became gentler (Fig. 8). Eventually the isopycnal became nearly flat at the depth of 430–450 m, while it became a little deeper at the center.

One of the key factors to deepen the interface is the freshwater accumulated in the BG that changes the dynamic height. The upper ocean has been becoming fresher since 2007. Much more freshwater accumulated in the upper ocean during 2008–11. The source of the freshwater is the large decrease of sea ice and input of more river runoff in the summertime (e.g., McLaughlin et al. 2011; Morison et al. 2012). The denser and saltier AW would flow to a deeper place when the upper ocean becomes fresher.

An increase in dynamic height during 2003 to 2011 indicates the spinup of the BG and accumulation of freshwater (McLaughlin and Carmack 2010) in the Canada basin (Fig. 9). Sea level height is higher in the spinup BG center and lower at the edge during sea ice retreat years compared to that in normal years (Giles et al. 2012). The increase in dynamic height is direct evidence that supports that the deepening of the isopycnal was induced by the enhanced BG and the addition of more freshwater. The spatial distribution of the dynamic height indicates the position of the BG where the freshwater was piled up. The dynamic height increased sharply after 2007 and maintained the high value in the following

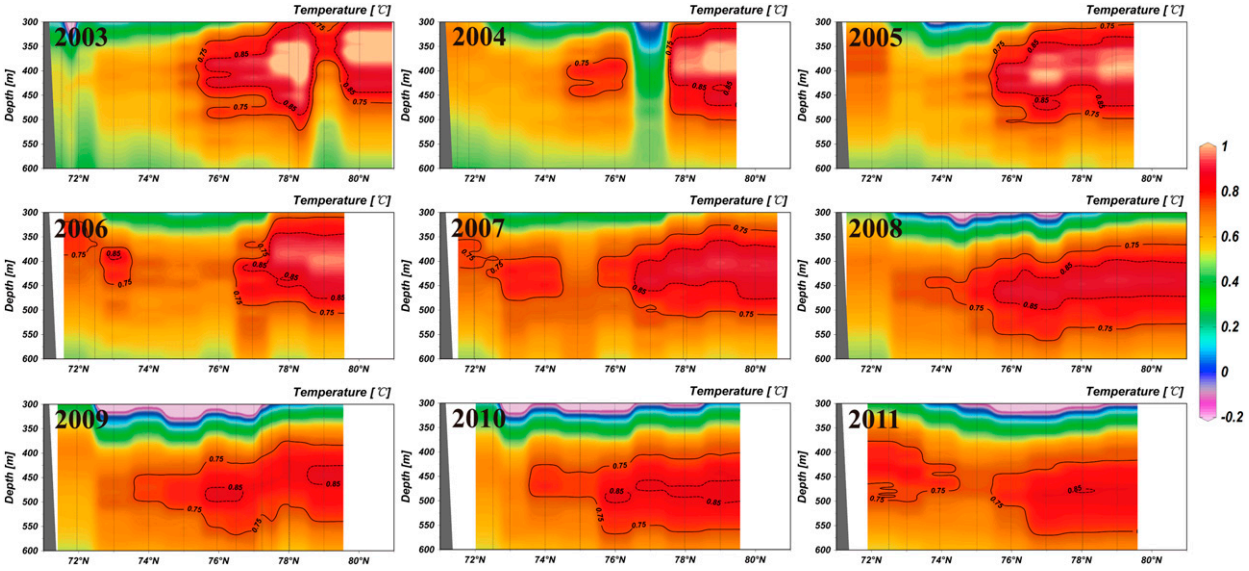

FIG. 5. Temperature of the western section (see Fig. 1 for its location). The thin black lines mark the locations of the CTD casts. The thick solid and dashed contours are for 0.75° and 0.85°C, respectively.

years. The change of circulation results in the release of freshwater in the BG that alters the dynamic height of 2009 and 2011, which was smaller than the previous year.

4. Impact of surface stress curl on the deepening of the AW

The fundamental factor for the spinup of the BG is the enhanced negative surface stress curl. The increase in surface stress could be due to two factors: (i) stronger winds and (ii) faster sea ice drift (e.g., Giles et al. 2012). The latter can be due to the less compact, thinner ice as the sea ice cover retreats or due to the increased air–ice and ice–ocean drag coefficients caused by higher ice roughness (e.g., Tsamados et al. 2014).

Figure 10a shows the annual-mean surface stress curl anomaly from 1995 to 2011 in the Canada basin. Before 2003, the annual surface stress curl was mainly positively anomalous; after that, the negative phase dominated, especially in 2007 (with the exception of 2006). Since the hydrographic survey was carried out in the summer, it is

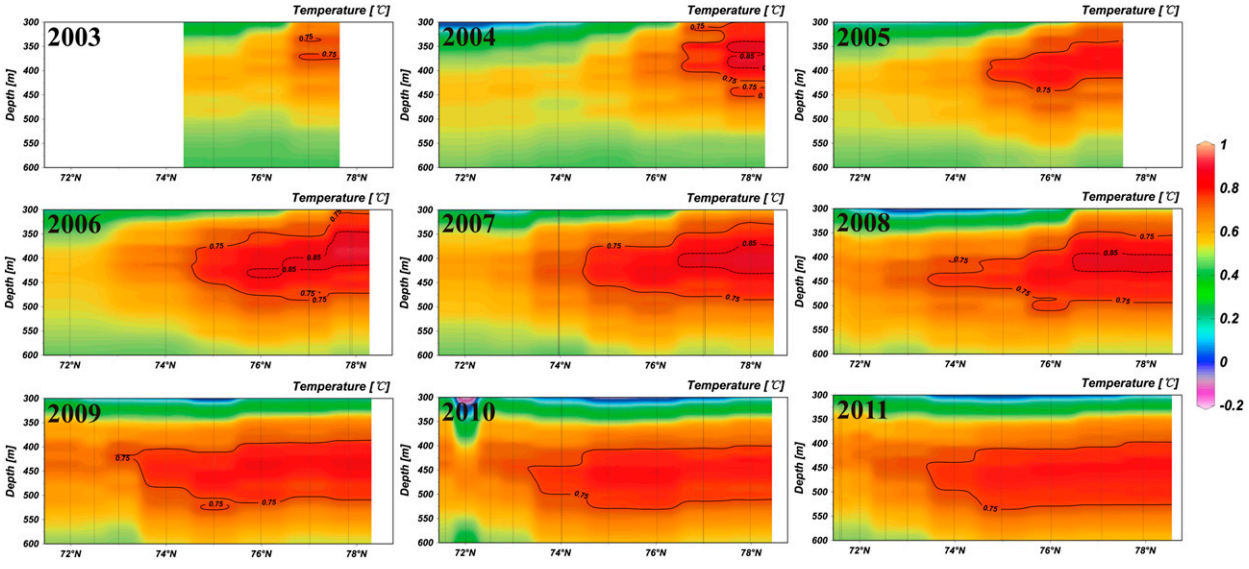

FIG. 6. As in Fig. 5, but for the eastern section (see Fig. 1 for its location).

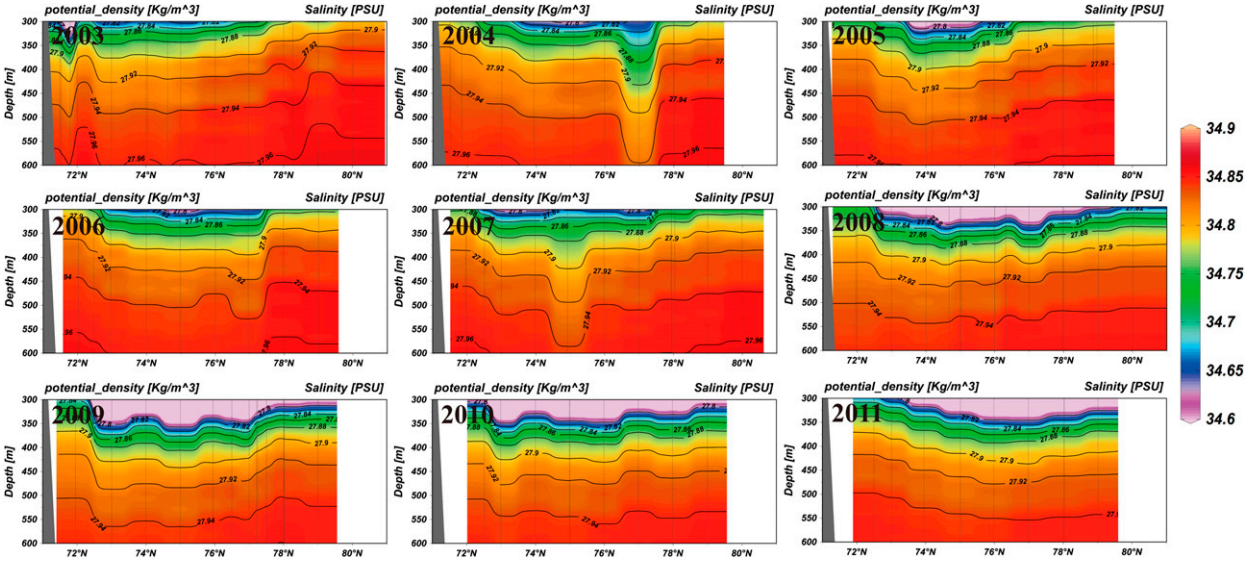

FIG. 7. Density (contours) and salinity (shadings) of the western section. The thin black lines mark the locations of the CTD casts.

more suitable to use the average of summer surface stress curl (in this study we used the July to September average value) to estimate the effect of it to the deepening of the AW core or dynamic height (Fig. 10b). The trend of the surface stress curl shows that much stronger surface stress appeared in the southwestern Canada basin (Fig. 10c). The change in surface stress curl greatly supported the deepening described in this study, under which the spinup of the BG and higher dynamic height could happen. The change in the water column height results in a change of interface depth and hence the change in the AWCD (Morison et al. 2012). The area mean of total surface stress in the Canada basin shows the increasing trend of the convergence of surface water. What is more, the area of the maximum increasing trend of Ekman pumping velocity is coincident with the deepening center area of the AWCD (figure not shown). It shows a large increase in downward Ekman pumping, emphasizing the importance of atmospheric forcing in the recent accumulation of freshwater and the deepening of the AW core in the Canada basin. Although the surface stress curl in some years decline after 2007, the dynamic height continues to increase as the freshwater continues to accumulate in the BG that then deepens the AW core.

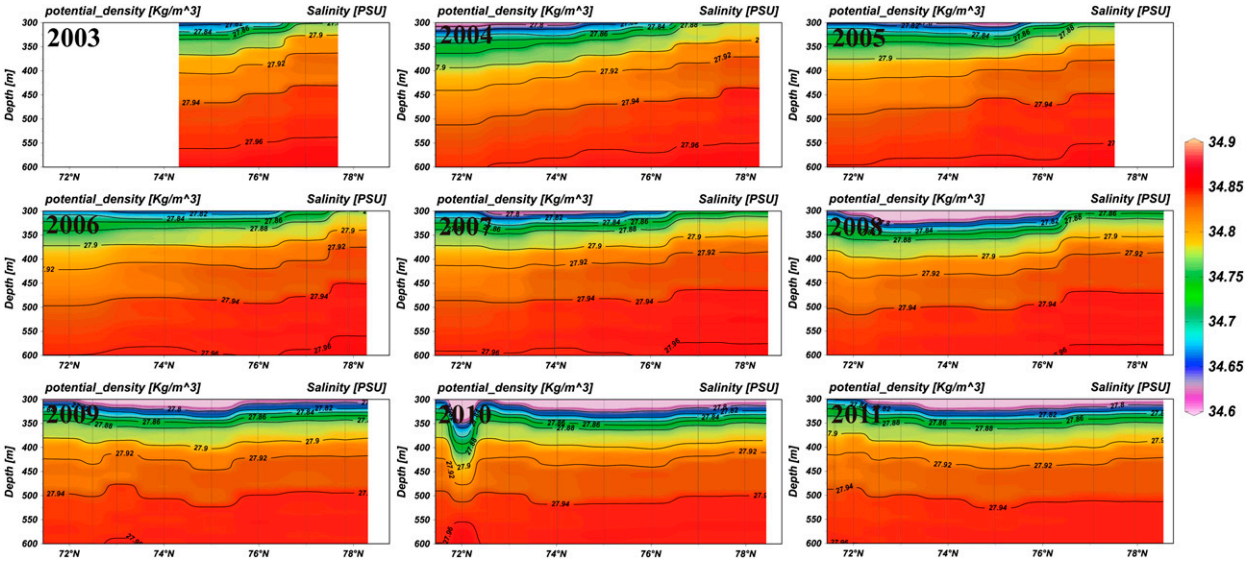

FIG. 8. As in Fig. 7, but for the eastern section.

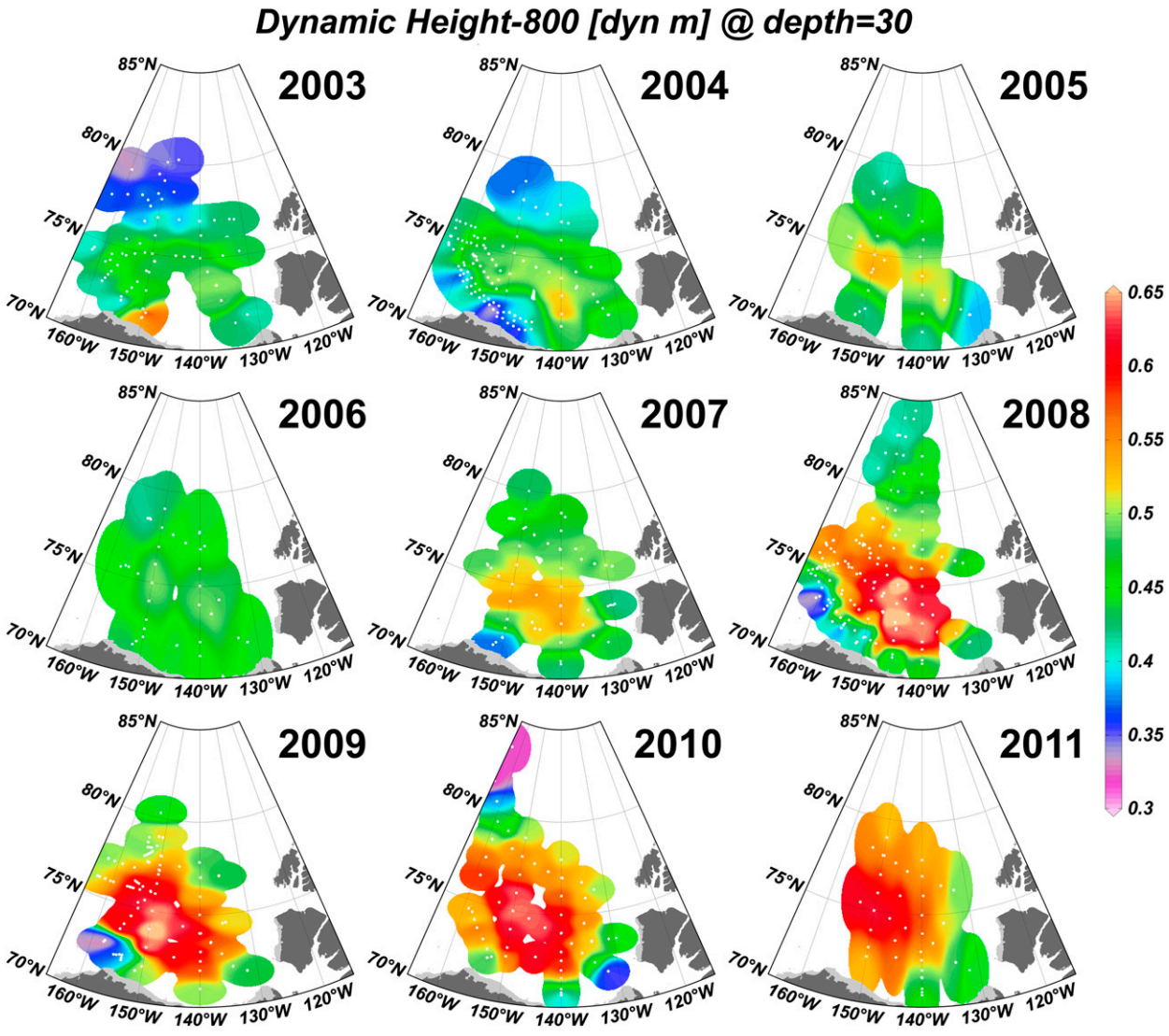

FIG. 9. Dynamic height (m) at 30 m in the Canada basin, calculated using 800 m as the reference depth. The white dots indicate the locations where the CTD data were collected, and the values between stations are interpolated.

Figure 9 shows that the position of the BG has moved to the southwestern part of the Canada basin since 2007, where a large ice-free area appeared. The sea ice experienced a rapid decline in the summertime of the last 10 yr. The black line in Fig. 4 shows the minimum of the sea ice edge from 2003 to 2011, which maintained low values with extensive ice-free areas. The most obvious reduction in sea ice appeared in the southwestern Canada basin. Both the wind stress and ice–ocean stress show an increasing trend based on our calculation. Our results confirmed the result of Yang (2009) that the acceleration was not driven solely by the wind stress. However, the change in ice dynamics (thinner and less areal coverage) was responsible for the change of the ice velocity, and thus the increase of surface stress. The first-year sea ice is more sensitive to the wind forcing than the multiyear sea ice. The first-year sea ice replaced most of the multiyear ice in the southern Canada basin (Kwok et al. 2009; Hutchings and Rigor 2012). The sea ice movement was strengthened under the condition of more extensive ice-free area and thinner first-year ice (Rampal et al. 2009; Spreen et al. 2011). What is more, retreating of the sea ice in summer contributes to more freshwater content in the upper ocean. Therefore, the direct consequence of sea ice retreat is the increase of surface stress curl (negatively) (Fig. 10), which then reinforces the convergence of the BG and accumulation of freshwater in summer.

Whether the surface stress was enhanced by stronger wind itself or due to the retreat of sea ice (stronger sea

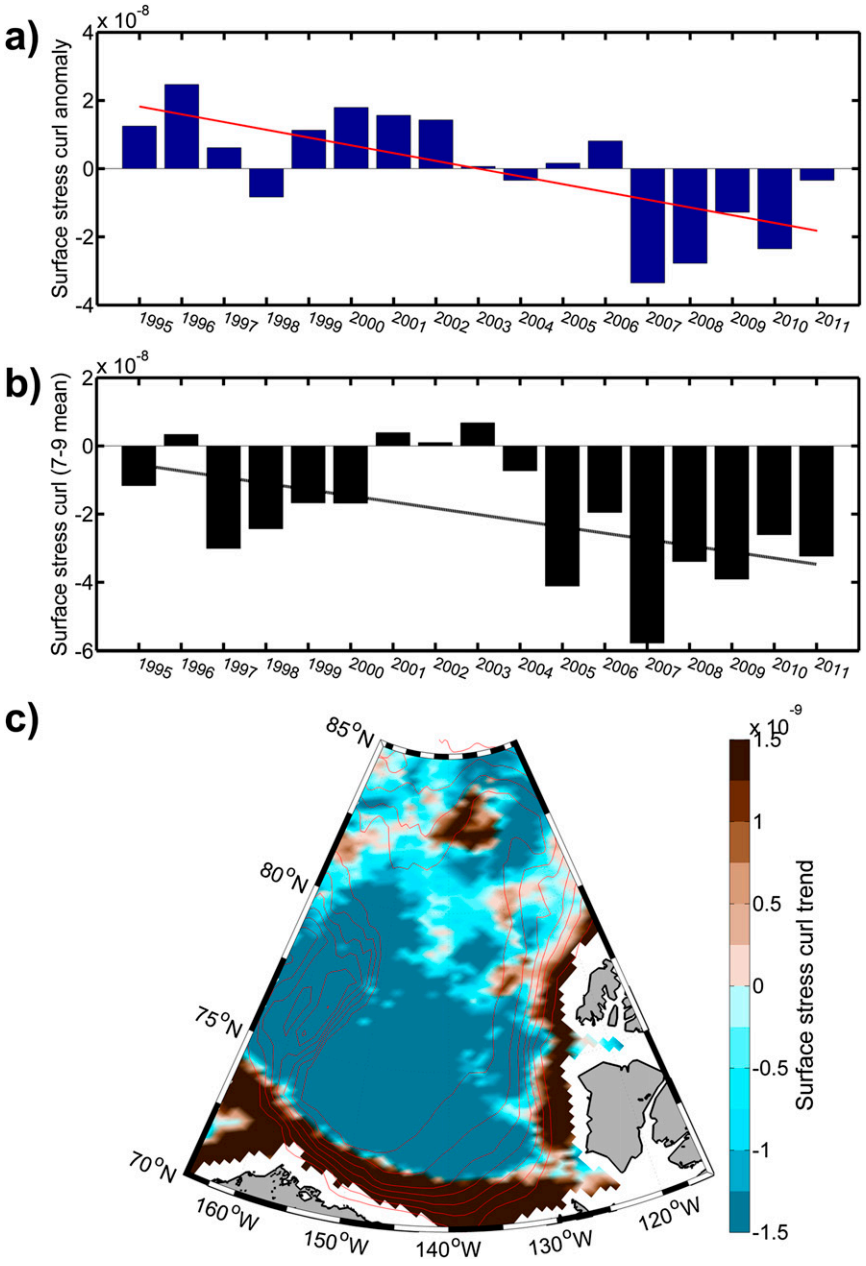

FIG. 10. (a) Annual-mean surface stress curl anomaly ($\mathrm{N\,m^{-3}}$) in the Beaufort Gyre (average over the Beaufort Gyre region bounded by the dashed line in Fig. 1). (b) July to September mean surface stress curl. (c) Trend of the surface stress curl in the Canada basin (1995–2011) calculated from the NCEP–NCAR reanalysis data, sea ice motion, and sea ice concentration data. The depth contours in red are schematic, ranging from 500 to 3500 m at an interval of 500 m.

ice motion), the enhanced surface stress curl will result in a deepening of the AW core. Impacts of surface stress curl on the AWCD could be estimated using a 2.5-layer (reduced gravity) model (see the appendix for detail). The variation in h_1 (thickness of upper ocean) impacted by surface stress curl (curl $\boldsymbol{\tau}$) can be estimated using the equation

$$\Delta h_1 \approx fL\Delta\boldsymbol{\tau}/(k_1 g_1'), \tag{1}$$

where the friction coefficient $k_1 = 2.5 \times 10^{-2}$ is derived from Firing et al. (1999), the reduced gravity is $g_1' = g(\rho_2 - \rho_1)/\rho_0 = 5 \times 10^{-2}\,\mathrm{m\,s^{-2}}$, and the Coriolis parameter is $f = 1.5 \times 10^{-4}\,\mathrm{s^{-1}}$. If the surface stress is $\Delta\boldsymbol{\tau} = 10^{-3}\,\mathrm{N\,m^{-2}}$ (derived from Fig. 10) and the length

scale of BG is $L = 5 \times 10^5$ m, the increased surface stress curl can lead to a deepening of the AW core by 60 m.

This result indicates that the enhanced surface stress curl can induce a deepening in the center of the BG. The enhanced surface stress curl could be a combination of the intensified negative wind stress curl and intensified sea ice motion as the sea ice retreat. If the enhanced surface stress curl continues, the AW core inside the BG would maintain in a deeper place.

5. Transition of density versus depth relationship

The result in section 3 indicates that the cooling of the AW could induce a deepening of the AW core, while the conclusion in section 4 indicates that the enhanced surface stress curl can also result in a deepening of the AW core. Here, we combine the impacts of these two factors in order to reveal the transition mechanism of the relatively shallow AW core to the deepened AW core in the Canada basin.

As illustrated in Fig. 3, by 2009 the deepened AW core region had spread over most of the survey area of the Canada basin. We investigate the relationship between density and depth of AW core [hereinafter referred to as the density versus depth (DVD) relationship] in the region influenced by the BG. Before doing so, the extent of the Beaufort Gyre needs to be identified roughly in order to select the stations. A method similar to that suggested by Jackson et al. (2011) is adopted. The isohalines in the anticyclonic BG has a bowl shape, with isohalines deeper at the center and shallower at the edge. So the isolines could be used to identify the shape of the BG and the depth of isohalines could be used to estimate the scope of the BG. Considering the decreasing salinity trend in the upper ocean of the Canada basin in recent years (Proshutinsky et al. 2009; McLaughlin et al. 2011), the same isohaline could not be used each year for comparative purposes (Jackson et al. 2011). The depth of a different isohaline for each year is chosen to determine the BG-dominated area and the location of BG (Fig. 11a). The stations that are inside the BG are defined as the region where the depth of the chosen isohaline is ranging from 25 to 45 m. By plotting the depth of the chosen isohaline, the location of the BG became a variable and appeared to be in the east Canada basin in 2003, in the southeast Canada basin in 2004, in the central basin in 2005, 2006 and 2007, in the south basin in 2008, in the southwest Canada basin in 2009 and 2010, and in the west of the basin in 2011. The clustered black dots that represent those stations that are inside the BG in the DVD relationship of AW core are linearly fitted, as shown in Fig. 11b.

Before 2007, the linear fit for the DVD scatterplot in the BG interior shows a negative slope, which is the denser water being deeper and lighter water being shallower characteristics of the line (Fig. 11b), which indicates that the AWCD was mainly dominated by density. In 2003 and 2004, the density of the AW core ranged from 27.90 to 27.95 kg m^{-3}, while the depth range was from 325 to 450 m. By the year 2007, the DVD relationship for the stations inside the BG was closely clustered, which looks like a transition year. The linearly fitted line for the stations inside the BG appeared as a positive slope in 2008, indicating a characteristic of the case when the denser water was shallower and the case when the lighter water was deeper. Meanwhile, the spatial variation of the density of AW core was reduced and clustered around 27.92–27.93 kg m^{-3}, but the maximum spatial difference of the AWCD was still within 50–60 m. In 2008, some stations distributed in the southwestern and western basin are shown as blue squares. The linearly fitted line for these stations still maintained a negative slope in 2008, implying that outside of the BG the AWCD was still controlled by the changing density. However, the slope of the linearly fitted line of stations inside the BG has become positive since 2008 and remained the same sign in the following years during our study period (Fig. 11b). In most years the fitted lines are past the 95% significance level. In 2007, the significant level is 90%. The fitted lines in 2005 and 2006 are lower than 90% significant level due to the sparse survey stations in 2005 and 2006. In fact, the variation of AWCD might not arise by density (temperature). The other processes including the surface freshwater, mixing during their flowing, and so on might contribute to the AWCD variation. Nevertheless, the variation of AWCD with these mechanisms all results in a negative slope before 2008 in the DVD relation figures, as they are highly relevant to the source water that flows into the basin. The low significance level during 2005–07 suggests that they probably are transition years, during which the DVD relationship changed from negative slope to positive slope. The most attractive feature to us is the slope changes to positive (or nearly vertical), which indicates there is something going on beside the thermodynamic process.

The characteristic DVD relationship of the case when the denser water was shallower and the case when the lighter water was deeper is obviously not induced by the density of the AW. As indicated in section 4, the spinup of the anticyclonic BG would result in increasing dynamic height, and thus isohalines much deeper in the center and relatively shallow at the edge, which is the main reason for the slope of the fitted line to be positive. In the center of the intensified BG, the AW core was depressed, though the AW inside the gyre was still warmer, forming the case when the lighter water is at the deeper

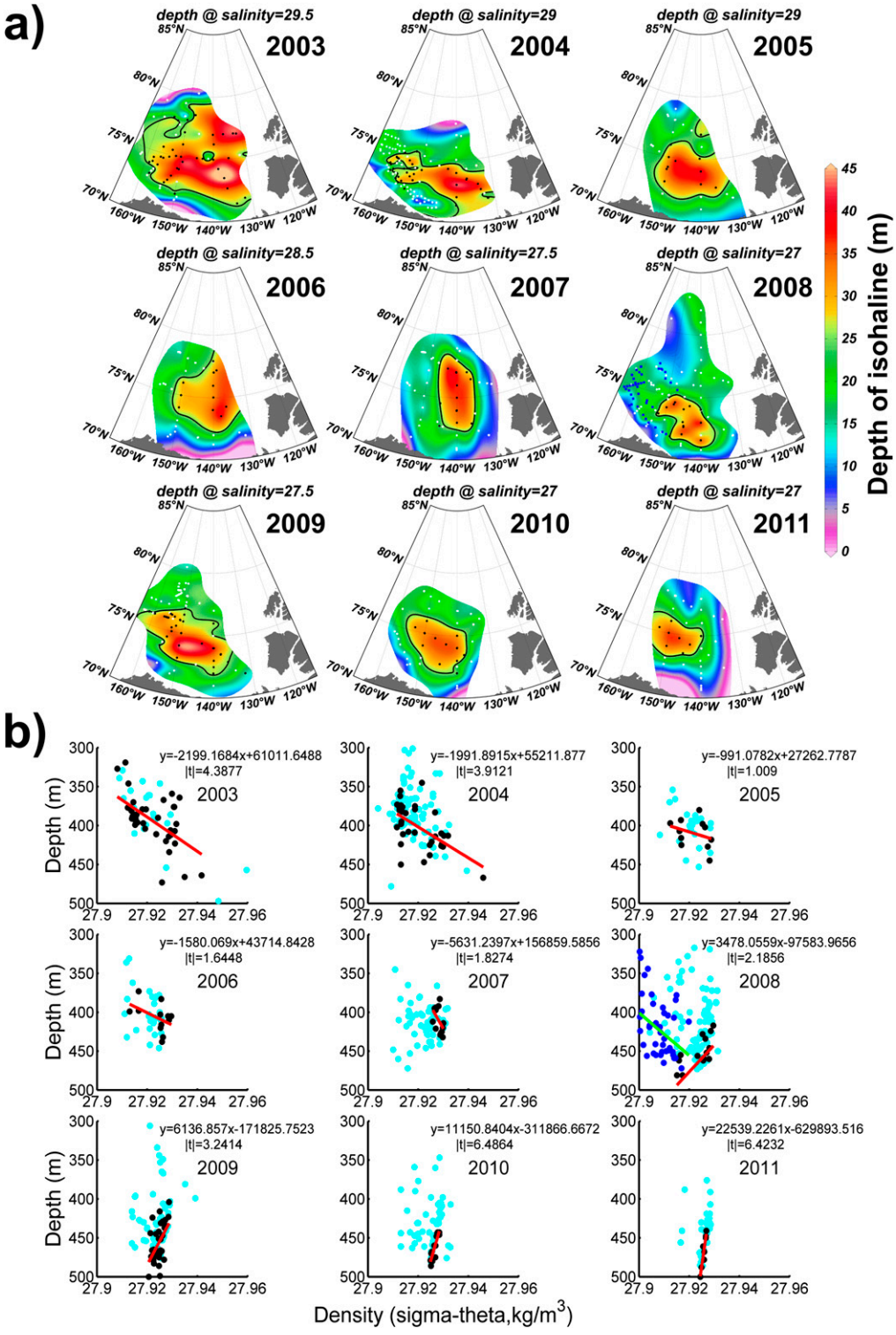

FIG. 11. (a) The Beaufort Gyre area (circled by 25-m isoline) determined by the depth of a chosen isohaline. The isohaline is 29.5 in 2003; 29 in 2004 and 2005; 28.5 in 2006; 27.5 in 2007 and 2009; and 27.0 in 2008, 2010, and 2011. Black dots represent the stations that were inside the Beaufort Gyre, white dots represent the stations that were outside the gyre, and blue squares represent the stations outside the gyre that were used for the linear-fitted line in 2008. (b) Density vs depth of the AW core relationship. The black and cyan dots represent the stations that were inside and outside the Beaufort Gyre, respectively. The red lines are fitted for the black dots inside the gyre. The fitted green line in 2008 is for the blue squares in the margin of the southwestern Canada basin (outside the gyre).

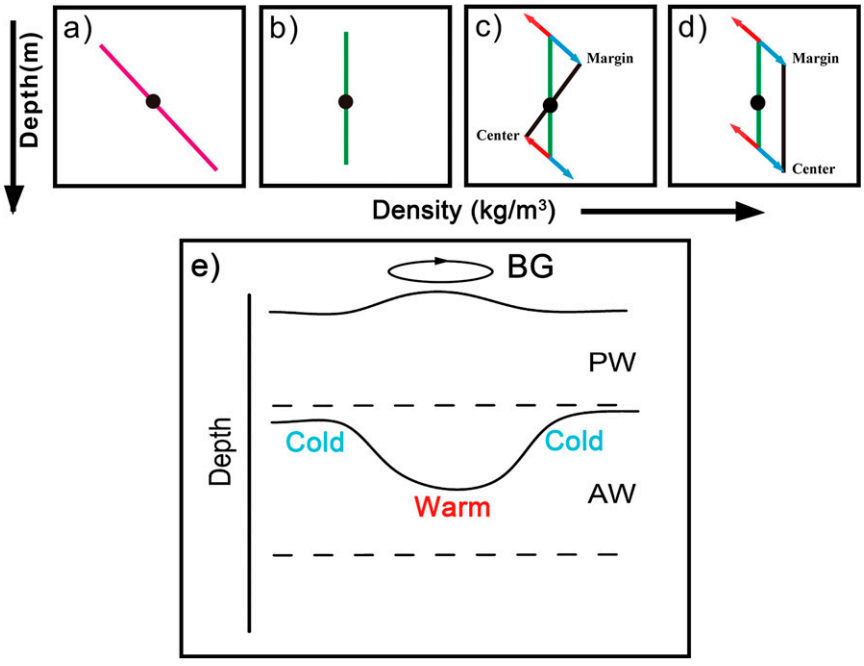

FIG. 12. Schematic views of possible types of density vs depth relationship of the AW: (a) Type 1, (b) Type 2, (c) Type 3, (d) Type 4, detail refers to the text in section 5. (e) The DVD relationship changing mechanism. BG refers to the Beaufort Gyre, PW refers to Pacific Water, and AW refers to Atlantic Water. The word warm in red refers to the warm AW, while the word cold in blue refers to the relatively cold AW. The word center refers to stations that are near the BG center, while margin refers to the stations that are near the BG margin.

end of the fitted line. While at the edge of the intensified BG, the AWCD would be relatively shallow; though, it was becoming colder and denser, forming the case when the denser water is at the shallower end of the fitted line. The enhancement of the BG was caused by the intensified negative surface stress curl. The surface convergence of enhanced BG increased the dynamic height and resulted in the freshwater pool at the top of the water column.

The reversed DVD relationship since 2008 can only exist with lighter (warmer) AW inside the gyre and denser (colder) AW at the edge. The results show the slightly colder AW only reached the edge of the BG (Fig. 11a), while inside the gyre it was still controlled by relatively warm AW (Fig. 4). The year 2007 is regarded as a transitional time for the DVD relationship to change from the phase with a negative slope to that with a positive slope.

The above conclusions could be illustrated by a simple sketch in Fig. 12, which gives the possible types of DVD relationship of the AW. In an ideal case, when the density is uniform spatially and there is neutral surface stress, all the AWCD will cluster at a black dot in Fig. 12a (Type 1). The black dot is used to illustrate all the stations around the basin cluster together. The variation in DVD relationship can be generalized to three types: 1) when there are vast thick ice covers, the AWCD is mainly controlled by density, and the DVD relationship varies along the line in Fig. 12a (Type 1) in a negative slope (as the case before 2007). It should be noted that the negative fitted slope is not only determined by the density of AW core but also influenced by the changing density of the total water column above the AW. 2) In an ideal case when the density of the AW is a constant around the basin, the enhanced surface stress caused by enhanced wind or sea ice motion can lead to a perpendicularly fitted line (Fig. 12b; Type 2), because in this case, the AW core is deeper at the center and shallower at the margin. 3) In the case of sea ice retreat that favors the increase of surface stress curl, if the colder/warmer AW only reaches the margin of the BG, the AW depth will vary along the upper blue/red arrows in Fig. 12c (Type 3). On the other hand, if the colder/warmer AW reaches the center of the gyre, the depth will vary along the lower blue/red arrows in Fig. 12c. The joint effects of surface stress and density variations are determined by the black line linking the ends of the arrows. Since 2007, the sea ice started tremendous retreating in the southern Canada basin, and a positive fitted slope was induced by the increase of surface stress curl, accumulation of freshwater, and colder AW at the periphery of the gyre.

Based on the mechanisms discussed above, it is reasonable to project that the slope of the fitted line would become more perpendicular in the future if the trend of sea ice declining continues (Stroeve et al. 2012) and the warm AW in the central BG will eventually be replaced by slightly colder AW in the future. The fitted line would be a ligature between the two blue arrows as the black line shows in Fig. 12d (Type 4; more perpendicular). Therefore, the DVD relationship is always important for identifying depth variation of the AW and the main driving factors.

6. Discussion and conclusions

The variability of AWCD in the Canada basin during 2003–11 was investigated in this study. It is shown that the AWCD in most survey areas of the Canada basin was shallower than 350 m in 2003, except of a rather deep AWCD area in the southeastern basin. Since then, the relatively deep AWCD area continued to expand. The deepening area marked by 410-m contour was extended from east to west during 2003–05 and then from south to north during 2006–11. Up to 2009, almost all the survey area of the Canada basin was filled with deepened AW. The cooling process that happened in the northwestern Canada basin is an interesting phenomenon. We think this cooling is relating to the inflow of slightly colder AW. The mechanism of this arrival of slightly colder AW is associated with what happened in the upstream along the flow pathway of the circumpolar boundary current. The onslope shift of the warmer AW jet was observed in response to the offslope (winter) wind (Dmitrenko et al. 2010). We hypothesize that the increase of Ekman transport (offslope) in recent years would result in the compensation of a warmer AW jet to the continental shelf that releases more heat to the upper layer and atmosphere, like the Laptev Sea and the eastern Siberian Sea. Thus, the AW lost much more heat than before when it flowed into the Canada basin. It is also may be a function of AW transport rate, that is, it is transported more slowly and thus had more time to cool via intrusions.

We considered the combined effects of density and sea ice retreating in this study. At the periphery of the BG, the colder AW tended to deepen the AW core. At the center of the gyre, the AW was relatively warm and should be shallower, but the enhanced surface stress and increasing freshwater content in the upper ocean results in increasing dynamic height that displaces the isopycnals downward (see the schematic mechanism shown in Fig. 12e). So, the impact of warmer AW was contrary to that caused by change in the negative surface stress curl. When the influence of temperature overwhelmed that of the surface stress curl and before the increase of the freshwater content period, the slope of the linearly fitted line was negative (Fig. 11b), that is, the case when the denser water is deeper and the case when the lighter water is shallower that appeared (before 2007). Contrarily, when the impact of surface stress curl, increasing freshwater content, and the spinup of the BG (McLaughlin et al. 2011; Giles et al. 2012) overwhelmed that of temperature, the slope turned to be positive, which is the denser water being shallower and the lighter water being deeper pattern that became dominant after 2008. The DVD relationship could be a useful tool to confirm the dominant factor for the change of AWCD by analyzing varying possible slopes.

The deepening of the AW benefits the reservation of the heat stored in the AW. The less release of the heat from the AW would negatively feed back to the sea ice retreat. Also, the reserved heat in the AW would be transported over a longer distance. The intensified BG that forces on the AW would change the structure of the Circumpolar Boundary Current and eventually influence the outflow to the Fram Strait. Our conclusions are mainly based on the data that were acquired after the 1990s anomalously warm AW flowed into the Canada basin and during a period that favored anticyclonic atmospheric and oceanic circulations and a larger ice-free area in the basin at summertime. The recent anticyclonic circulation regime started in 1997, persisted through 2012 and lasted over 16 yr (except for 2009), instead of the typical 5–8 yr (Timmermans et al. 2012). So our conclusions are fundamentally based on terms of the circulation regime in the Canada basin, because of the data that are available to us. The conclusions are concert with the strength of BG in the Canada basin. When the Arctic Ocean swaps to the cyclonic regime, the BG is weaker and the impact of the BG to depress the AW core would become weaker. It also should be noted that a second anomalously warm AW flowed into the Arctic Ocean that reached its highest in 2006 (Polyakov et al. 2011, 2012); we would expect that the DVD relationship would return to show a negative slope when it arrived in the Canada basin with relatively cold AW inside the BG, while another warm AW was in the margin. Further observations are needed to help us better understand the dynamics between the upper-ocean conditions and the interior ocean structure.

Acknowledgments. This study was supported by the National Project of China for Global Change Research (2010CB951403) and the Project for Arctic and Antarctic Expedition (CHINARE2012-04-03). The authors thank Prof. Jiuxin Shi and Dr. Xiang Li for their insightful discussions. We are greatly indebted to the scientists and

technicians at WHOI, DFO, CHINARE, and JAMSTEC who carried out the field expeditions. Several figures were produced using Ocean Data View (R. Schlitzer 2013, Ocean Data View data; http://odv.awi.de). Comments from three anonymous reviewers were valuable and have greatly improved the manuscript.

APPENDIX

The Relationship between the Surface Stress Curl and Depth of AW Core

Using a 2.5-layer (reduced gravity) model, we try to evaluate the impact of surface stress curl on the AWCD. The first model layer represents the upper ocean above the halocline (in the Canada basin, the halocline above the Atlantic Water is at about 200 m), the second layer represents the Atlantic Water, and the deeper layer is assumed to be motionless. The thicknesses of the upper-ocean layer and the AW layer are h_1 and h_2, respectively. The change in AWCD can be represented by the change in h_1. The vertical integration of momentum and continuity equations of the top- and middle layer is

$$\begin{aligned} -fV_1 &= -g(h_1+\zeta)\frac{\partial \zeta}{\partial x}+\frac{\tau_{xw}}{\rho_1}-\frac{\tau_{x1}}{\rho_1}\\ fU_1 &= -g(h_1+\zeta)\frac{\partial \zeta}{\partial y}+\frac{\tau_{yw}}{\rho_1}-\frac{\tau_{y1}}{\rho_1}, \quad \text{and}\\ \frac{\partial U_1}{\partial x}&+\frac{\partial V_1}{\partial y}=0 \end{aligned} \tag{A1}$$

$$\begin{aligned} -fV_2 &= \left(-g\frac{\partial \zeta}{\partial x}+g_1'\frac{\partial h_1}{\partial x}\right)(h_2-h_1)+\frac{\tau_{x1}}{\rho_2}-\frac{\tau_{x2}}{\rho_2}\\ fU_2 &= \left(-g\frac{\partial \zeta}{\partial y}+g_1'\frac{\partial h_1}{\partial y}\right)(h_2-h_1)+\frac{\tau_{y1}}{\rho_2}-\frac{\tau_{y2}}{\rho_2},\\ \frac{\partial U_2}{\partial x}&+\frac{\partial V_2}{\partial y}=0 \end{aligned} \tag{A2}$$

where the reduced gravity is $g_1'=g(\rho_2-\rho_1)/\rho_0$ and $g_2'=g(\rho_3-\rho_2)/\rho_0$. The term ρ is the water density for each layer, and we use the approximation $\rho_1\simeq\rho_2\simeq\rho_0$; g is the gravity, and f is the Coriolis parameter; U and V are the vertically integrated velocities; ζ is the sea surface elevation; τ_{xw} and τ_{yw} are surface stress components; and $\tau_{x1}(\tau_{y1})$ and $\tau_{x2}(\tau_{y2})$ are the interfacial shear stress between upper-middle and middle-bottom layers, respectively. Following Firing et al. (1999), we use

$$\begin{aligned} \tau_{x1}&=k_1(U_1/h_1-U_2/h_2);\\ \tau_{y1}&=k_1(V_1/h_1-V_2/h_2), \quad \text{and} \end{aligned} \tag{A3}$$

$$\tau_{x2}=(k_2U_2)/h_2; \quad \tau_{y2}=(k_2V_2)/h_2, \tag{A4}$$

where k_1 is the friction coefficient. Based on the above equations, the relationship between surface stress and h_1 could be derived from

$$\frac{\partial^2 h_1}{\partial x^2}+\frac{\partial^2 h_1}{\partial y^2}=\frac{\mathrm{div}\boldsymbol{\tau}}{\rho_1 g_1' h_1}+\frac{f\,\mathrm{curl}\boldsymbol{\tau}}{k_1 g_1'}. \tag{A5}$$

The surface stress divergence is the same order of magnitude with surface stress curl ($10^{-8}\,\mathrm{N\,m^{-3}}$) based on our calculation, but the coefficient of divergence in the first term on the right side of Eq. (A5) is much less than the coefficient of curl in the second term ($10^{-4}\ll 0.12$) based on the value of the parameters in the equation. So the first term is able to be neglected, compared to the second term. The variation of h_1 impacted by surface stress can be estimated from Eq. (A5), that is,

$$\Delta h_1\approx fL\Delta\boldsymbol{\tau}/(k_1 g_1'), \tag{A6}$$

where the friction coefficient $k_1=2.5\times10^{-2}$, derived from Firing et al. (1999) with the consideration of the velocity near the core layer being $\sim$4.86 cm s^{-1} (Shimada et al. 2004a). The reduced gravity is $g_1'=g(\rho_2-\rho_1)/\rho_0=5\times10^{-2}\,\mathrm{m\,s^{-2}}$, and the Coriolis parameter is $f=1.5\times10^{-4}\,\mathrm{s^{-1}}$. If the surface stress is $\Delta\boldsymbol{\tau}=10^{-3}\,\mathrm{N\,m^{-2}}$ (derived from Fig. 10) and the length scale of BG is $L=5\times10^5$ m, the increased surface stress curl can lead to a deepening of the AW core by 60 m.

REFERENCES

Aksenov, Y., V. V. Ivanov, A. J. G. Nurser, S. Bacon, I. V. Polyakov, A. C. Coward, A. C. Naveira-Garabato, and A. Beszczynska-Moeller, 2011: The Arctic Circumpolar Boundary Current. *J. Geophys. Res.,* **116,** C09017, doi:10.1029/2010JC006637.

Carmack, E. C., and Coauthors, 1997: Changes in temperature and tracer distributions within the Arctic Ocean: Results from the 1994 Arctic Ocean section. *Deep-Sea Res. II,* **44,** 1487–1502, doi:10.1016/S0967-0645(97)00056-8.

Dmitrenko, I. A., and Coauthors, 2009: Seasonal modification of the Arctic Ocean intermediate water layer off the eastern Laptev Sea continental shelf break. *J. Geophys. Res.,* **114,** C06010, doi:10.1029/2008JC005229.

——, and Coauthors, 2010: Impact of the Arctic Ocean Atlantic Water layer on Siberian shelf hydrography. *J. Geophys. Res.,* **115,** C08010, doi:10.1029/2009JC006020.

Firing, E., B. Qiu, and W. Miao, 1999: Time-dependent island rule and its application to the time-varying North Hawaiian Ridge Current. *J. Phys. Oceanogr.,* **29,** 2671–2688, doi:10.1175/1520-0485(1999)029<2671:TDIRAI>2.0.CO;2.

Fowler, C., W. Emery, and M. Tschudi, 2013: Polar Pathfinder Daily 25 km EASE-Grid Sea Ice Motion Vectors, version 2. National Snow and Ice Data Center, Boulder, CO, digital media. [Available online at http://nsidc.org/data/nsidc-0116.]

Giles, K. A., S. W. Laxon, A. L. Ridout, D. J. Wingham, and S. Bacon, 2012: Western Arctic Ocean freshwater storage increased by

wind-driven spin-up of the Beaufort Gyre. *Nat. Geosci.,* **5,** 194–197, doi:10.1038/ngeo1379.

Hutchings, J. K., and I. G. Rigor, 2012: Role of ice dynamics in anomalous ice conditions in the Beaufort Sea during 2006 and 2007. *J. Geophys. Res.,* **117,** C00E04, doi:10.1029/2011JC007182.

Iselin, C. O'D., 1939: The influence of vertical and lateral turbulence on the characteristics of the waters at mid-depths. *Trans. Amer. Geophys. Union,* **20,** 414–417.

Ivanov, V. V., and Coauthors, 2009: Seasonal variability in Atlantic Water off Spitsbergen. *Deep-Sea Res. I,* **56,** 1–14, doi:10.1016/j.dsr.2008.07.013.

Jackson, J. M., S. E. Allen, F. A. McLaughlin, R. A. Woodgate, and E. C. Carmack, 2011: Changes to the near-surface waters in the Canada basin, Arctic Ocean from 1993–2009: A basin in transition. *J. Geophys. Res.,* **116,** C10008, doi:10.1029/2011JC007069.

Kalnay, E., and Coauthors, 1996: The NCEP/NCAR 40-Year Reanalysis Project. *Bull. Amer. Meteor. Soc.,* **77,** 437–471, doi:10.1175/1520-0477(1996)077<0437:TNYRP>2.0.CO;2.

Kwok, R., G. F. Cunningham, M. Wensnahan, I. Rigor, H. J. Zwally, and D. Yi, 2009: Thinning and volume loss of the Arctic Ocean sea ice cover: 2003–2008. *J. Geophys. Res.,* **114,** C07005, doi:10.1029/2009JC005312.

Lenn, Y. D., and Coauthors, 2009: Vertical mixing at intermediate depths in the Arctic boundary current. *Geophys. Res. Lett.,* **36,** L05601, doi:10.1029/2008GL036792.

Lique, C., and M. Steele, 2012: Where can we find a seasonal cycle of the Atlantic Water temperature within the Arctic basin? *J. Geophys. Res.,* **117,** C03026, doi:10.1029/2011JC007612.

——, J. D. Guthrie, M. Steele, A. Proshutinsky, J. H. Morison, and R. Krishfield, 2014: Diffusive vertical heat flux in the Canada basin of the Arctic Ocean inferred from moored instruments. *J. Geophys. Res. Oceans,* **119,** 496–508, doi:10.1002/2013JC009346.

McLaughlin, F., and E. C. Carmack, 2010: Deepening of the nutricline and chlorophyll maximum in the Canada basin interior, 2003–2009. *Geophys. Res. Lett.,* **37,** L24602, doi:10.1029/2010GL045459.

——, ——, R. W. MacDonald, A. J. Weaver, and J. Smith, 2002: The Canada basin 1989–1995: Upstream events and far-field effects of the Barents Sea. *J. Geophys. Res.,* **107,** doi:10.1029/2001JC000904.

——, K. Shimada, E. C. Carmack, M. Itoh, and S. Nishino, 2005: The hydrography of the southern Canada basin, 2002. *Polar Biol.,* **28,** 182–189, doi:10.1007/s00300-004-0701-6.

——, E. C. Carmack, S. Zimmerman, D. Sieberg, L. White, J. Barwell-Clarke, M. Steel, and W. K. W. Li, 2008: Physical and chemical data from the Canada basin, August 2004. Canadian Data Rep. of Hydrography and Ocean Sciences 140, 185 pp.

——, ——, W. J. Williams, S. Zimmermann, K. Shimada, and M. Itoh, 2009: Joint effects of boundary currents and thermohaline intrusions on the warming of Atlantic Water in the Canada basin, 1993–2007. *J. Geophys. Res.,* **114,** C00A12, doi:10.1029/2008JC005001.

——, ——, A. Proshutinsky, R. A. Krishfield, C. Guay, M. Yamamoto-Kawai, J. M. Jackson, and B. Williams, 2011: The rapid response of the Canada basin to climate forcing: From bellwether to alarm bells. *Oceanography,* **24,** 146–159, doi:10.5670/oceanog.2011.66.

McPhee, M. G., A. Proshutinsky, J. H. Morison, M. Steele, and M. B. Alkire, 2009: Rapid change in freshwater content of the Arctic Ocean. *Geophys. Res. Lett.,* **36,** L10602, doi:10.1029/2009GL037525.

Morison, J., R. Kwok, C. Peralta-Ferriz, M. Alkire, I. Rigor, R. Andersen, and M. Steele, 2012: Changing Arctic Ocean freshwater pathways. *Nature,* **481,** 66–70, doi:10.1038/nature10705.

Ostrom, W., J. Kemp, R. Krishfield, and A. Proshutinsky, 2004: Beaufort Gyre freshwater experiment: Deployment operations and technology in 2003. Woods Hole Oceanographic Institute Tech. Rep. WHOI-2004–01, 32 pp.

Polyakov, I. V., and Coauthors, 2004: Variability of the intermediate Atlantic Water of the Arctic Ocean over the last 100 years. *J. Climate,* **17,** 4485–4497, doi:10.1175/JCLI-3224.1.

——, and Coauthors, 2005: One more step toward a warmer Arctic. *Geophys. Res. Lett.,* **32,** L17605, doi:10.1029/2005GL023740.

——, and Coauthors, 2010: Arctic Ocean warming contributes to reduced polar ice cap. *J. Phys. Oceanogr.,* **40,** 2743–2756, doi:10.1175/2010JPO4339.1.

——, and Coauthors, 2011: Fate of early 2000s Arctic warm water pulse. *Bull. Amer. Meteor. Soc.,* **92,** 561–566, doi:10.1175/2010BAMS2921.1.

——, A. V. Pnyushkov, and L. A. Timokhov, 2012: Warming of the intermediate Atlantic Water of the Arctic Ocean in the 2000s. *J. Climate,* **25,** 8362–8370, doi:10.1175/JCLI-D-12-00266.1.

Proshutinsky, A. Y., and M. A. Johnson, 1997: Two circulation regimes of the wind-driven Arctic Ocean. *J. Geophys. Res.,* **102,** 12 493–12 514, doi:10.1029/97JC00738.

——, R. H. Bourke, and F. A. McLaughlin, 2002: The role of the Beaufort Gyre in Arctic climate variability: Seasonal to decadal climate scales. *Geophys. Res. Lett.,* **29,** 2100, doi:10.1029/2002GL015847.

——, and Coauthors, 2009: Beaufort Gyre freshwater reservoir: State and variability from observations. *J. Geophys. Res.,* **114,** C00A10, doi:10.1029/2008JC005104.

Quadfasel, D. A., A. Sy, D. Wells, and A. Tunik, 1991: Warming in the Arctic. *Nature,* **350,** 385, doi:10.1038/350385a0.

Rampal, P., J. Weiss, and D. Marsan, 2009: Positive trend in the mean speed and deformation rate of Arctic sea ice, 1979–2007. *J. Geophys. Res.,* **114,** C05013, doi:10.1029/2008JC005066.

Rudels, B., H. J. Freidrich, and D. Quadfasel, 1999: The Arctic circumpolar boundary current. *Deep-Sea Res. II,* **46,** 1023–1062, doi:10.1016/S0967-0645(99)00015-6.

Schauer, U., R. D. Muench, B. Rudels, and L. Timokhov, 1997: Impact of eastern Arctic shelf waters on the Nansen basin intermediate layers. *J. Geophys. Res.,* **102,** 3371–3382, doi:10.1029/96JC03366.

——, and Coauthors, 2002: Confluence and redistribution of Atlantic Water in the Nansen, Amundsen and Makarov basins. *Ann. Geophys.,* **20,** 257–273, doi:10.5194/angeo-20-257-2002.

Shimada, K., F. McLaughlin, E. Carmack, A. Proshutinsky, S. Nishino, and M. Itoh, 2004a: Penetration of the 1990s warm temperature anomaly of Atlantic Water in the Canada basin. *Geophys. Res. Lett.,* **31,** L20301, doi:10.1029/2004GL020860.

——, S. Nishino, and M. Itoh, 2004b: R/V *Mirai* cruise report. Joint Western Arctic Climate Studies Rep. MR04-05, 112 pp. [Available online at http://www.godac.jamstec.go.jp/catalog/data/doc_catalog/media/MR04-05_all.pdf.]

Spreen, G., L. Kaleschke, and G. Heygster, 2008: Sea ice remote sensing using AMSR-E 89-GHz channels. *J. Geophys. Res.,* **113,** C02S03, doi:10.1029/2005JC003384.

——, R. Kwok, and D. Menemenlis, 2011: Trends in Arctic sea ice drift and role of wind forcing: 1992–2009. *Geophys. Res. Lett.,* **38,** L19501, doi:10.1029/2011GL048970.

Stroeve, J., M. Serreze, M. Holland, J. Kay, J. Malanik, and A. Barrett, 2012: The Arctic's rapidly shrinking sea ice cover: A research synthesis. *Climatic Change,* **110,** 1005–1027, doi:10.1007/s10584-011-0101-1.

Swift, J. H., E. P. Jones, K. Aagaard, E. C. Carmack, M. Hingston, R. W. MacDonald, F. A. McLaughlin, and R. G. Perkin, 1997:

Waters of the Makarov and Canada basins. *Deep-Sea Res. I,* **44,** 1503–1529, doi:10.1016/S0967-0645(97)00055-6.

Timmermans, M.-L., J. Toole, R. Krishfield, and P. Winsor, 2008: Ice-tethered profiler observations of the double-diffusive staircase in the Canada basin thermocline. *J. Geophys. Res.,* **113,** C00A02, doi:10.1029/2008JC004829.

——, and Coauthors, cited 2012: Ocean. Arctic report card: Update for 2012, NOAA. [Available online at http://www.arctic.noaa.gov/report12/ocean.html.]

Tsamados, M., D. Feltham, D. Schroeder, D. Flocco, S. Farrell, N. Kurtz, S. Laxon, and S. Bacon, 2014: Impact of variable atmospheric and oceanic form drag on simulations of Arctic sea ice. *J. Phys. Oceanogr.,* **44,** 1329–1353, doi:10.1175/JPO-D-13-0215.1.

Woodgate, R. A., K. Aagaard, J. H. Swift, W. M. Smethie Jr., and K. K. Falkner, 2007: Atlantic Water circulation over the Mendeleev Ridge and Chukchi Borderland from thermohaline intrusions and water mass properties. *J. Geophys. Res.,* **112,** C02005, doi:10.1029/2005JC003416.

Yang, J., 2005: The Arctic and subarctic ocean flux of potential vorticity and the Arctic Ocean circulation. *J. Phys. Oceanogr.,* **35,** 2387–2407, doi:10.1175/JPO2819.1.

——, 2009: Seasonal and interannual variability of downwelling in the Beaufort Sea. *J. Geophys. Res.,* **114,** C00A14, doi:10.1029/2008JC005084.

Zhang, J., D. A. Rothrock, and M. Steele, 1998: Warming of the Arctic Ocean by a strengthened Atlantic inflow: Model results. *Geophys. Res. Lett.,* **25,** 1745–1748, doi:10.1029/98GL01299.

Zhang, Y., and J. Zhao, 2007: The estimation of vertical turbulent diffusivity in the surface layer in the Canada basin (in Chinese with English abstract). *Periodical Ocean Univ. China,* **37,** 695–703.

Zhao, J., G. Gao, and Y. Jiao, 2005: Warming in Arctic intermediate and deep waters around Chukchi Plateau and its adjacent regions in 1999. *Sci. China Ser. D Earth Sci.,* **48,** 1312–1320, doi:10.1360/02yd0504.